



DOI: 10.5604/01.3001.0053.8486

Synthesis of metallic alloy particles on flat graphitic interfaces in arc discharge

A. Breus*, S. Abashin, O. Serdiuk, Iu. Sysoiev

Plasma Laboratory, Faculty of Aircraft Engines, National Aerospace University, Kharkiv 61070, Ukraine

* Corresponding e-mail address: A.Breus@khai.edu

ORCID identifier:  <https://orcid.org/0000-0002-7310-1465> (A.B.)

ABSTRACT

Purpose: The application of arc discharge to synthesising encapsulated (Fe-Cu-Al)@C structures is studied. The cost-effectiveness of the proposed technique may be beneficial for developing a new method for large-scale production of metal micro- and nanoparticles protected from oxidation by a carbon shell.

Design/methodology/approach: A copper sample was immersed into a mixture of graphite, iron, and aluminium powder and placed into a negatively powered crucible of a setup designed to ignite arc discharge at atmospheric conditions. The proposed approach prevents the oxidation of droplets of Fe-Cu-Al alloy by covering them with a thin layer of carbon, which is also engaged as a collector of the metal particles.

Findings: The application of arc discharge resulted in the generation of metal particles and various carbon nanostructures, which were confirmed by SEM images. The nanostructures were grouped into more complex flower-, ball-, tree-, and octopus-shaped structures with a large yield of metallic alloy particles ranging from a few μm (micrometers) to nanometre sizes. These findings suggest the catalytic application of the structures after the grown particles are cleared from the carbon shell to be implemented as active chemical agents.

Research limitations/implications: The main limitation is the uncontrolled heat transfer from the discharge volume. Therefore, an additional screen should be installed around the volume in order to improve control over synthesis in future studies.

Practical implications: This research confirms a flexible and simple method of synthesising metallic alloy particles that may be applied for catalytic applications.

Originality/value: The synthesis is conducted using a well-known arc discharge technique to expand the production yield and diversity of chemically-active metal particles protected from oxidation by a shell before the intended application.

Keywords: Nanotechnology, Arc discharge, Micro- and nanoparticles, Alloy

Reference to this paper should be given in the following way:

A. Breus, S. Abashin, O. Serdiuk, Iu. Sysoiev, Synthesis of metallic alloy particles on flat graphitic interfaces in arc discharge, Archives of Materials Science and Engineering 121/2 (2023) 49-59. DOI: <https://doi.org/10.5604/01.3001.0053.8486>

MATERIALS



1. Introduction

Nowadays, multi- and bimetallic, and metal oxide particles [1,2] are of great interest due to their potential application in medicine [3], solar cells [4], catalysis, and electronic devices [5], as well as green energy applications [6,7]. The shape, size, chemical composition, and electrical and magnetic properties of the particles allow for obtaining various synergetic effects, thus creating novel nanomaterials with outstanding properties. Magnetorheological fluids significantly increase their viscosity and become viscoelastic solids when exposed to a magnetic field [8]; Fe nanoparticles are considered to be good candidates to achieve this balance, but their implementation is hindered by the absence of an efficient preparation method. Superparamagnetic core-shell $\text{Fe}_3\text{O}_4@\text{SiO}_2$ -aminotet-Cu(II) nanoparticles were successfully generated chemically [9]. They can be recovered through the use of an external magnet and reused at least six times without any loss of their activity. Complex $\text{FeCoNiCrCuAl}_{0.3}$ microspheres shelled with Ni-NiO metal oxide have been successfully grown using a two-step hydrothermal method [10]. After studying the electromagnetic (EM) properties and EM wave absorption, it was found that the magnetic loss that arises from the interaction with the high-entropy alloy and the dielectric loss conditioned by Ni-NiO promoted the consumption of EM energy through a synergistic effect.

Various approaches can be used to develop an efficient strategy for structure preparation, starting from the treatment of chips [11] or control of internal stress [12]. A comprehensive review of strategies for nanoparticle synthesis was conducted by Lee *et al.* [13]. Even though thermal methods [14] are considered the simplest, their cost-effectiveness is poor due to the large production times compared to plasma-enhanced methods, which are widely applied for nanoparticle growth [15]. The advantages of plasma as a production tool originate from the flexible control over the charged particle distribution along the treated substrate [16]. Microwave discharge was used to grow Fe-cored carbon nanocapsules ($\text{Fe}@\text{CNCs}$), which showed extraordinary electromagnetic wave (EMW) absorption performance, thermos-oxidative stability, and anti-corrosion properties [17]. Radio-frequency reactive plasma was successfully implemented to conduct a highly controllable synthesis of CuO nanostructures [18].

Arc discharges are distinguished from electric discharges for their outstandingly high densities of plasma fluxes [19] and a single-step process (unlike chemical processes, which are usually multi-step, e.g.), which makes them a perfect candidate in nanoparticle fabrication; DC, AC, and pulsed discharges are engaged in that. Ashkarran *et al.* produced

fine and uniform ZrO_2 nanoparticles by submerging Zr electrodes into deionized water and observed that the size of the nanoparticles increased with increasing the DC arc current [20]. At the same time, the current change affected the band gap of the nanomaterial by shifting it from 5.4 eV at 10 A to 5 eV at 20 A. The same research group reported a process for synthesizing hybrid ZnO-Graphene nanostructures by passing an arc current between zinc electrodes in reduced graphene oxide (RGO) solution. The nanostructures significantly enhance the photodegradation of standard dyes under visible-light irradiation and can be excited by visible light, exhibiting considerable visible-light photocatalytic activity [21].

It should be mentioned that ecological issues are encountered while implementing arc technologies. Successful utilization of industrial wastes in eco-friendly manner to develop Cu (78 nm in diam.) and CuO nanoparticles (67 nm in diam.) suitable for various biomedical applications was demonstrated by Tharchanaa *et al.* [22] when applying the arc plasma discharge for copper scrap in N_2 and air gas mixture. Fe-Sn nanoparticles were prepared in vacuum by DC arc discharge (300 A) in a setup with a tungsten rod used as a cathode and Fe and Sn powders compressed into a cylindrical anode to be evaporated [23]. The high oxidation resistance in the air of the nanoparticles was explained by their shell/core structure with a SnO_2 shell of 5-10 nm in thickness.

However, using carbon-containing media for the synthesis is the most applied, primarily due to the necessity of protecting the formed metal particles from further oxidation. Arc-synthesized graphene-encapsulated iron nanoparticles ($\text{Fe}@\text{G}$) exhibited excellent catalytic performance in syngas conversion reaction, and the graphene shell is considered a protector for the iron core from oxidizing or acid etching [24]. Arc evaporation of Fe and SiC powders was applied to prepare C-Fe-Si alloy encapsulating Fe nanoparticles [25], and the alloyed shell exhibited protective properties for the core against air oxidation. Moreover, the magnetisation and coercivity were reduced by heat treatment after the arc synthesis. N-doped graphene layer-encapsulated NiFe bimetallic nanoparticles were synthesised by Qu *et al.* [26] in arc discharge to serve as a highly efficient microwave absorber. At that, magnetic NiFe alloy is advantageous in broadening the absorption bandwidth, while $\text{NiFe}@\text{C}$ composites efficiently increase corrosion resistance capability. Methane atmosphere was engaged to make FeCo and $\text{FeCo}@\text{C}$ nanoparticles in arc plasma, and the effect of core-shell nanostructure on absorbing and magnetic properties were investigated [27]. In addition to the protective properties, it was found that

FeCo@C nanoparticles show lower saturation magnetisation, followed by perfect impedance matching and reflection loss in the GHz frequency range, compared with FeCo nanoparticles. The effective complementarities between dielectric and magnetic losses in FeCo@C nanoparticles explained the effect.

Moreover, the application of carbon chemicals is conditioned by the necessity of collecting the formed particles in a net to prevent them from spreading in the reactor. The nanoparticles often serve as nucleation centres to develop a net, so the whole process can be described as a positive feedback circuit where the carbon network is a host for the nanoparticles, which, in turn, are the nuclei to grow the carbon net. This schematic has been implemented in a number of experiments. The arc discharge route performed in the PdCl₂ solution was successfully applied to grow carbon nanotubes with Pd nanoparticles with a diameter of 3 nm [28]. The palladium nanoparticles were found to be encapsulated in the nanotubes, and the whole nanostructure is suitable for the possible fabrication of electronic devices and hydrogen storage. CuO/Ta₂O₅ core/shell crystalline nanoparticles were fabricated by the arc discharge in water [29]. Xu *et al.* [30] reported about Ni, Co and Fe nanoparticles encapsulated in carbon shells after the arc was applied in aqueous solutions of NiSO₄, CoSO₄ and FeSO₄. However, the use of liquids complicates the process, which is why there is a clear tendency to apply gas-phase environment.

The gaseous atmosphere at the constant pressure of 60 kPa under Ar:H₂=1:1 was employed to generate carbon-encapsulated iron nanoparticles by a carbon arc [31]. Measurements of yield, diameter distribution, graphitisation degree and magnetic properties show that Fe content in the anode is from 7.5 to 65 at.% completely controls these characteristics. At the same time, the discharge current affects the product morphology, diameter distribution and graphitisation degree, while the phase composition does not depend on either parameter. In the research carried out by El-khatib *et al.* [32], the nanocomposites of nano zinc oxides as a matrix phase and multiwall carbon nanotubes as a reinforcement (NZnO/MWCNTs) were synthesised in deionised water by AC arc discharge between the graphite and zinc electrodes of different geometry and size. It was found that at the discharge current of 15 A the diameter of MWCNTs was increased twice (from 7.3 nm to 15.18 nm) while the diameter of NZnO stayed almost constant (12.24 nm and 15.36 nm) at a two-fold increase of the size of the electrodes. A pulsed arc applied in a vacuum chamber evacuated below 10⁻³ Pa in a container filled with powders

was engaged to fabricate Pt and Pd nanoparticles made of Pt/Al₂O₃ and Pd/CeO₂ catalysts [33]. Graphite encapsulated nickel nanoparticles (Ni-GEM) were produced in a tungsten arc-discharge system, where the anode is a graphite crucible loaded with nickel shots. PF resin, benzene and cyclohexane vapours were combined in three combinations to serve as a carbon source, while a tapered tungsten rod of 10 mm diameter served as a cathode. DC arc of 120 A was applied, and Ni-GEM nanoparticles exhibited the inner structure: carbon shell of 5-10 nm and Ni core of 30-50 nm [34]. The arc discharge process followed by an annealing treatment conducted by Kuchi *et al.* [35] resulted in the growth of a well-integrated composite of Fe₃O₄ and single-wall carbon nanotubes (SWCNTs) exhibiting strong microwave absorption. A hollow pure graphite tube with a length of 160 mm, outer diameter of 6.4 mm and inner diameter of 3 mm was used as the carbon source that was filled with Fe wires and a mixed powder of Fe with graphite (1:1). The discharge was ignited in a hydrogen atmosphere for 20 min at a partial pressure of 5.3MPa. Then the product was annealed at 500°C in a nitrogen atmosphere for two h to oxidise Fe into Fe₃O₄. Ag-Fe-decorated single-walled carbon nanotubes with excellent antibacterial activity against Escherichia coli were prepared in a simple DC hydrogen arc one-step process (80 A in atmosphere H₂:Ar=4:6 at a pressure of 200 Torr). Ag and Fe nanoparticles exhibited 1-10 nm diameters and were deposited at the SWCNT growth during the arc discharge evaporation [36]. Spherical Co-Cr-Cu-Fe-Ni nanoparticles of about 80-120 nm in diameter were synthesised in an arc, and it was found that the body-centred cubic (BCC) phase increases with the decrease of Cu content in the nanoparticles. At that, the particles showed comparable soft magnetic features, and the magnetic coupling of Cu-rich explained the asymmetric characteristic face-centred cubic phase with a relatively hard magnetic BCC crystalline phase [37].

Further improvement of the arc technology is associated with implementing the magnetic field in the process. The instability and short duty cycle of arc discharge resulted in numerous attempts to develop technological setups based on the utilisation of magnetic fields to guide the arc motion and keep arcs in specified regions of evaporated samples [38]. In particular, Wang *et al.* proposed a cylindrical plasma generator with an axial magnetic field to get the magnetically stabilised gliding arc discharge (MSGAD) [39]. In addition to the study of arc plasma parameters such as arc voltage, rotation speed, electric field, excitation and rotational temperature and so on, nanoparticles of carbon black with a “crumpled paper sheet” structure were grown.

They have crystalline structure, and the crystallinity is improved with an increased magnetic field. The effect of different gaseous atmospheres was explored in the magnetically stabilised gliding arc discharge (MSGAD) to produce carbon nanoparticles via methane decomposition [40]. In pure CH_4 and Ar, a mixture of spherical carbon nanoparticles and graphene nanoflakes (GNFs) was formed. In He and H_2 , only highly crystalline GNFs with excellent thermal stability were grown. At the same time, in the N_2 atmosphere, a mixture of GNFs, disordered graphitic layers, and carbon nanodots were synthesised, and nitrogen-doped nanoparticles were found. It has been proposed that hydrogen atoms, in combination with high input power promote the formation of GNFs.

However, producing a net of 1D carbon nanostructures presents a challenge due to the difficulty of extracting nanoparticles from it. Moreover, the literature review suggests the need to shorten the production time and study the possibility of excluding the pump systems, which increase the production costs. That is why the present research is dedicated to developing a reliable, environment-friendly and cost-effective arc-based technology where the carbon-encapsulated metallic alloy particles are synthesised on a flat graphitic interface at atmospheric conditions.

2. Research methodology

To conduct the experiments, a mixture of graphite powder (diameter of particles less than $200\ \mu\text{m}$ and

thickness of about $1\ \mu\text{m}$), aluminium powder (diameter of particles less than $20\ \mu\text{m}$), and iron (diameter of particles less than $20\ \mu\text{m}$) was mixed at a weight ratio 80:1:2 in a crucible, which was made of AISI 1020 Low Carbon Steel (Fe $\sim 99.08\text{--}99.53\%$; C $\sim 0.17\text{--}0.230\%$; Mn $\sim 0.30\text{--}0.60\%$; P $\leq 0.040\%$; S $\leq 0.050\%$). The mixture was scanned by SEM facility to measure the average content of the species over an area of $500\ \mu\text{m} \times 500\ \mu\text{m}$, and the result was C $\sim 79\%$; O $\sim 18\%$; Fe $\sim 2\%$; Al $\sim 1.0\%$. Thus, the mixture included a rather large oxygen content bound in graphite, iron, and aluminium oxides. A positively shifted tong of a welding machine was connected to a copper sample (purity 99.98%) with a thickness of 2 mm and diameter of 25 mm, while a negatively shifted – to the crucible (Fig. 1a). Purity of the samples were selected according to the literature review of the samples used for similar experiments. Less pure material can significantly affect the results due to the influence of the impurities, which can serve as nucleation centres. Before the treatment, the samples were washed in distilled water and dried. Then they were immersed into an ultrasonic facility with isopropyl alcohol and washed for 90 seconds, and dried.

The copper sample was immersed to approximately 5 mm into the mixture, and the distance between the sample and the walls of the crucible was about 10 mm; then, the arc current of 160 A was applied during 2 minutes. The time of the experimental run was chosen after a preliminary investigation since over a longer time of the experiment the degeneration of structures into monolithic formations was observed.

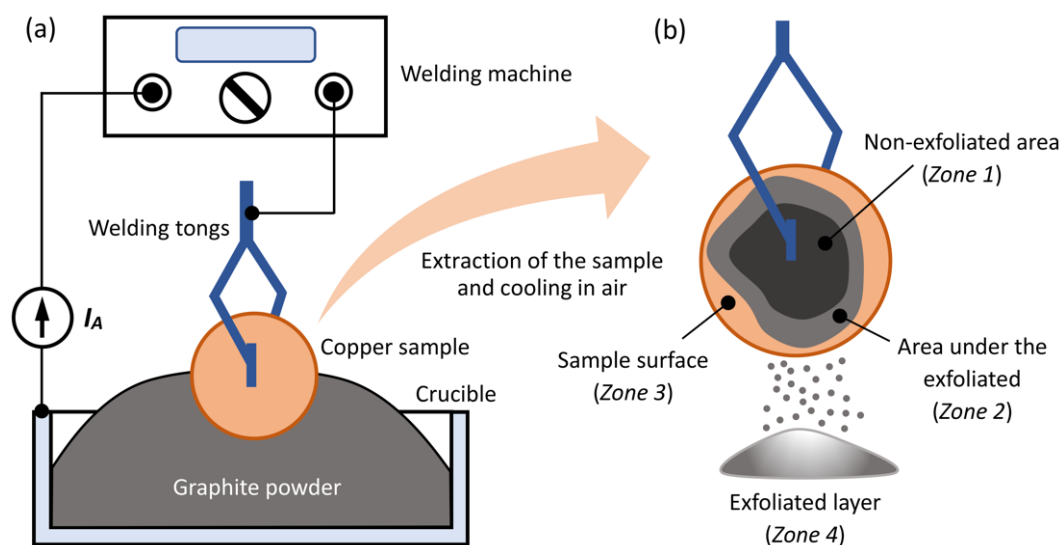


Fig. 1. Synthesis of complex nanoparticles in arc discharge: a) a schematic of the experimental setup; b) a schematic of the areas studied using SEM

Sparking was observed in the immersed part of the copper sample, and the mixture was heated red at that. The red glow was considered as evidence of heat radiation emitted by the mixture. Use of Thermalert® 4.0 Series Pyrometer measured the temperature of 820 C. There were ten experimental runs in a row; new sample, and the mixture of graphite, iron, and aluminium oxides were used each time. As a result of the treatment, the black layer was formed on surfaces of the copper samples. After the experiments, the samples were cooled in the atmosphere. At that, part of the black layer was exfoliated, so four typical zones in Figure 1b were distin-

guished. Then material from all zones underwent SEM studies to establish the morphology and elemental composition.

3. Research results and analysis

The experiments revealed the presence of a large diversity of structures obtained in the arc discharge initiated in the mixture. The general view of the structures observed in Zone 1 is presented in Figure 2a and shows a mixture of 2D microstructures covered with a number of smaller structures.

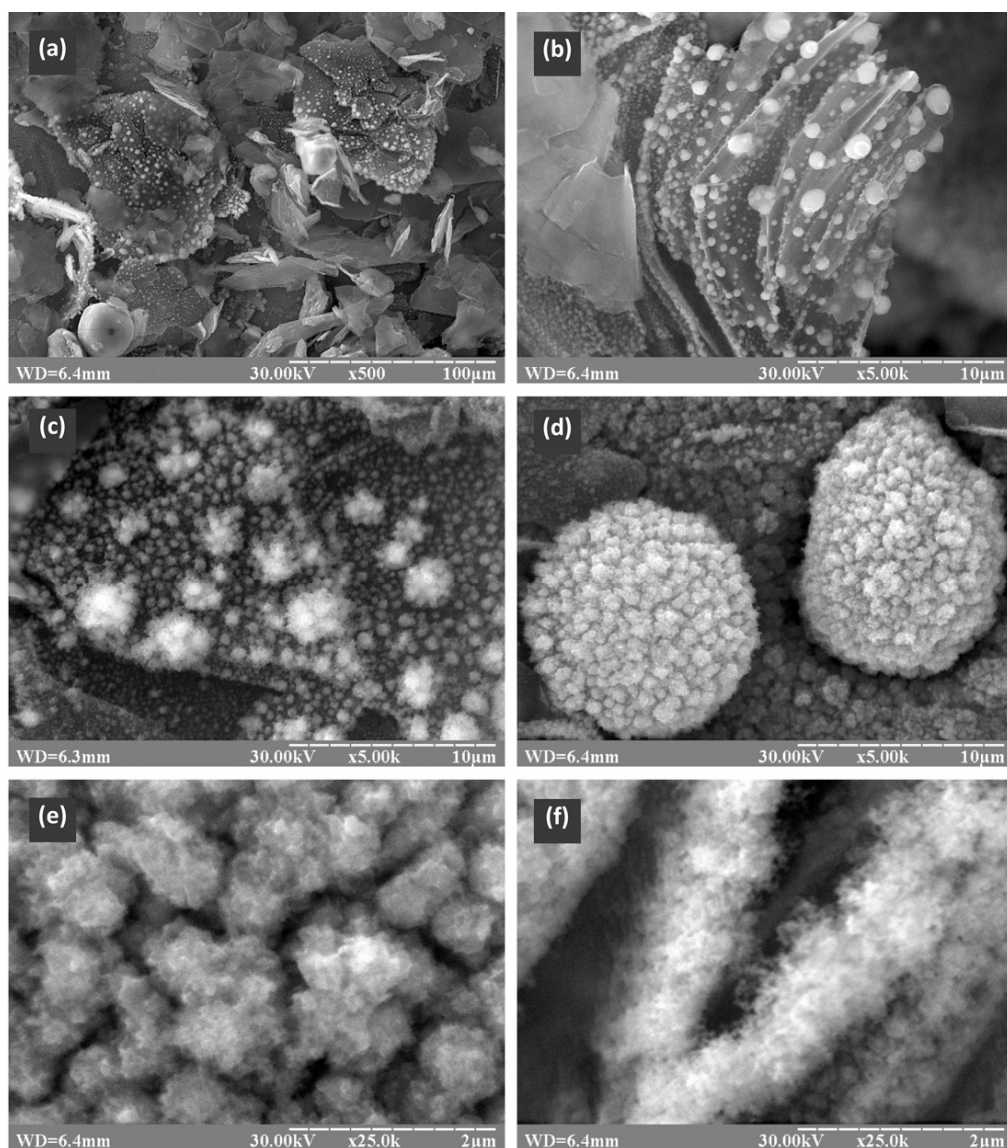


Fig. 2. SEM images of structures found in Zone 1 (ref. Fig. 1b): a) general view of the structures; b) wrinkled nanosheet with nanodots; c) nanoflowers with a size up to 2 μm ; d) balls with a diameter of about 10 μm ; e) magnified view of nanoballs; f) magnified view of complex 1D nanowires with a diameter of about 1 μm

Among these structures, wrinkled nanosheets are distinguishable, as it is shown in Figure 2b. An enhanced view of the small structures reveals nanoflowers with a size up to $2\ \mu\text{m}$ (Fig. 2c) and dots associated in microballs with a diameter of about $10\ \mu\text{m}$ (Fig. 2d). The magnified view of the microstructures allows resolving complex net-like structures composed of nanostructures (Fig. 2e), which can form 1D objects with a diameter of about $1\ \mu\text{m}$ (Fig. 2f).

While Zone 1 presents the layer that was saved from the exfoliation and stayed completely intact on the sample, Zone 2 shows the next layer under the partially exfoliated black layer. Here, the SEM image of the structures found in Zone 2 displays the general view of the structures (Fig. 3a), which are not only less abundant in comparison with the structures in Zone 1, but also have different appearance and are

presented by 2D structures with tree-like 1D nanostructures (Fig. 3b), and tree-like 1D nanostructures arranged in the octopus-like shape (Fig. 3c). Their magnified view is shown in Figure 3d which reveals the complex net-like nanostructure.

However, regarding the generation of complex nanoparticles, the most interesting results are obtained in Zone 4, which represents the exfoliated layer. The structures found in the deposit are shown in Figure 4. While the general view (Fig. 4a) of the powder shows just an array of disk-shaped microstructures with average size of $300\ \mu\text{m}$ in diameter and a few micrometres in thickness, a magnified view reveals the stacked 2D microstructure (Fig. 4b) that is also without traces of nanostructures. However, further magnification reveals 2D nanostructures with a size of about

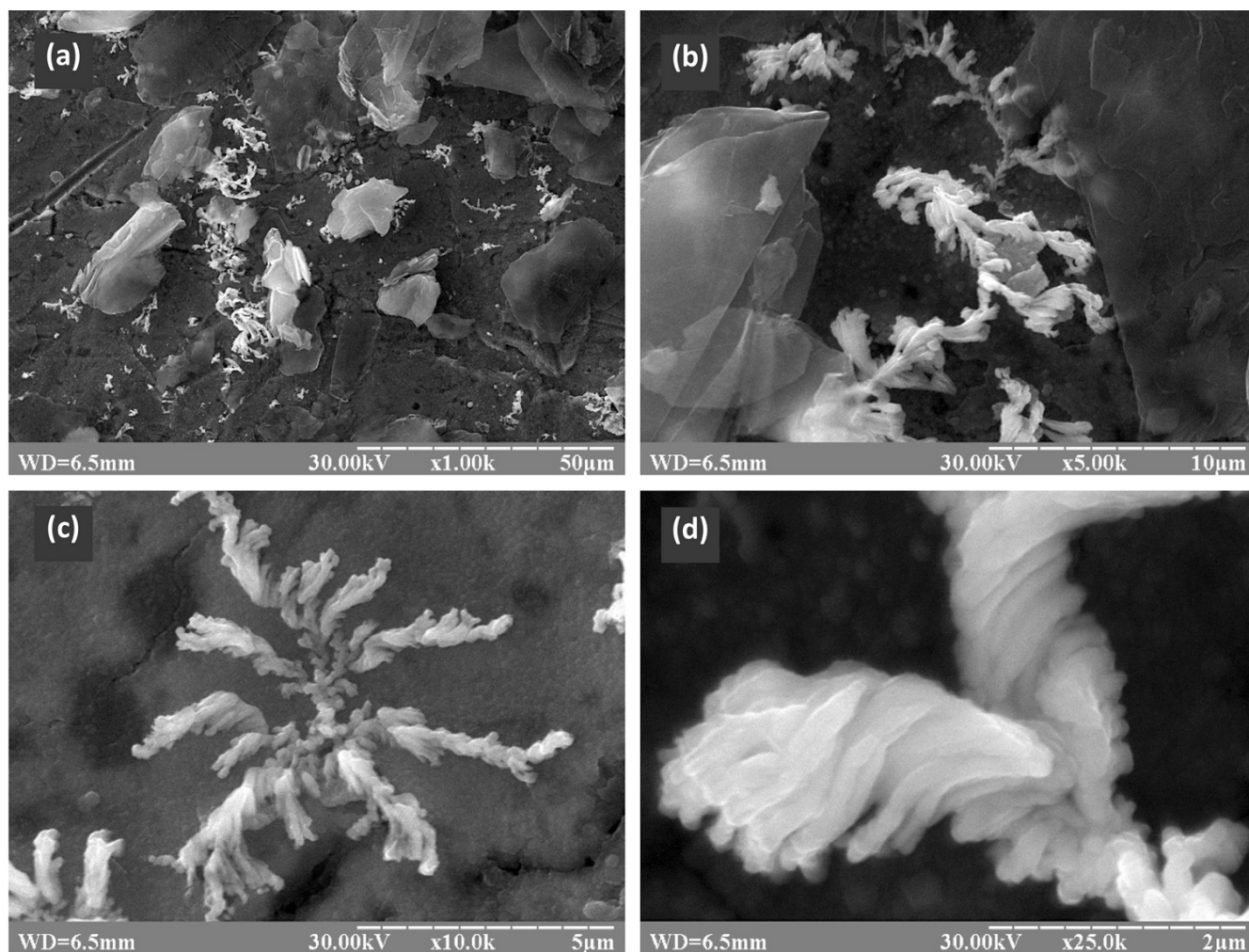


Fig. 3. SEM images of the structures found in Zone 2 (Ref. Fig. 1b): a) general view; b) 2D structures with tree-like 1D nanostructures; c) tree-like 1D nanostructures arranged in the octopus-like shape; d) magnified view of 1D nanostructure

40 μm in diameter and thickness of about 50 nm, covered by the micro- and nanodots (Fig. 4c, Fig. 4d). To characterise the elemental composition of the structures, five different regions were marked from 1 to 5 for further EDS analysis. The results of EDS analysis of the regions marked in Figure 4 are shown in Figure 5.

As it can be seen, the background region of the exfoliated powder reveals the presence of carbon (92.3%) with a small amount of oxygen (5.7%) copper (1.6%), and iron (0.4%); at that no traces of aluminium were detected (position 1). Thus, this region presents almost a pure graphite surface with traces of metals. When studying the surface of a graphite leaf (position 2) with the sizes of about 30 $\mu\text{m} \times 50 \mu\text{m}$, it was found that it is composed of carbon (88.8%) with a small

content of oxygen (8.1%) copper (2.2%), iron (0.6%), and aluminium (0.3%). Almost the same content of carbon, oxygen, copper, iron, and aluminium was found at another part of the leaf (position 3). These measurements allow us to conclude that the stable chemical composition of 2D nanostructures from one to another, and along the surface of the studied nano-leaf. As for the metal traces, the analysis of the droplets with a diameter of 2 μm (position 4) and diameter of 3 μm (position 5) on the surface revealed that the metals are concentrated in the droplets with almost the same elemental composition of about of 5-10% of carbon, 0.6-6.0% of oxygen, 15-26% of copper, 54-78% of iron, and 1-4% of aluminium. As it can be seen, the quantities of the elements differ mostly with respect to iron-copper ratio;

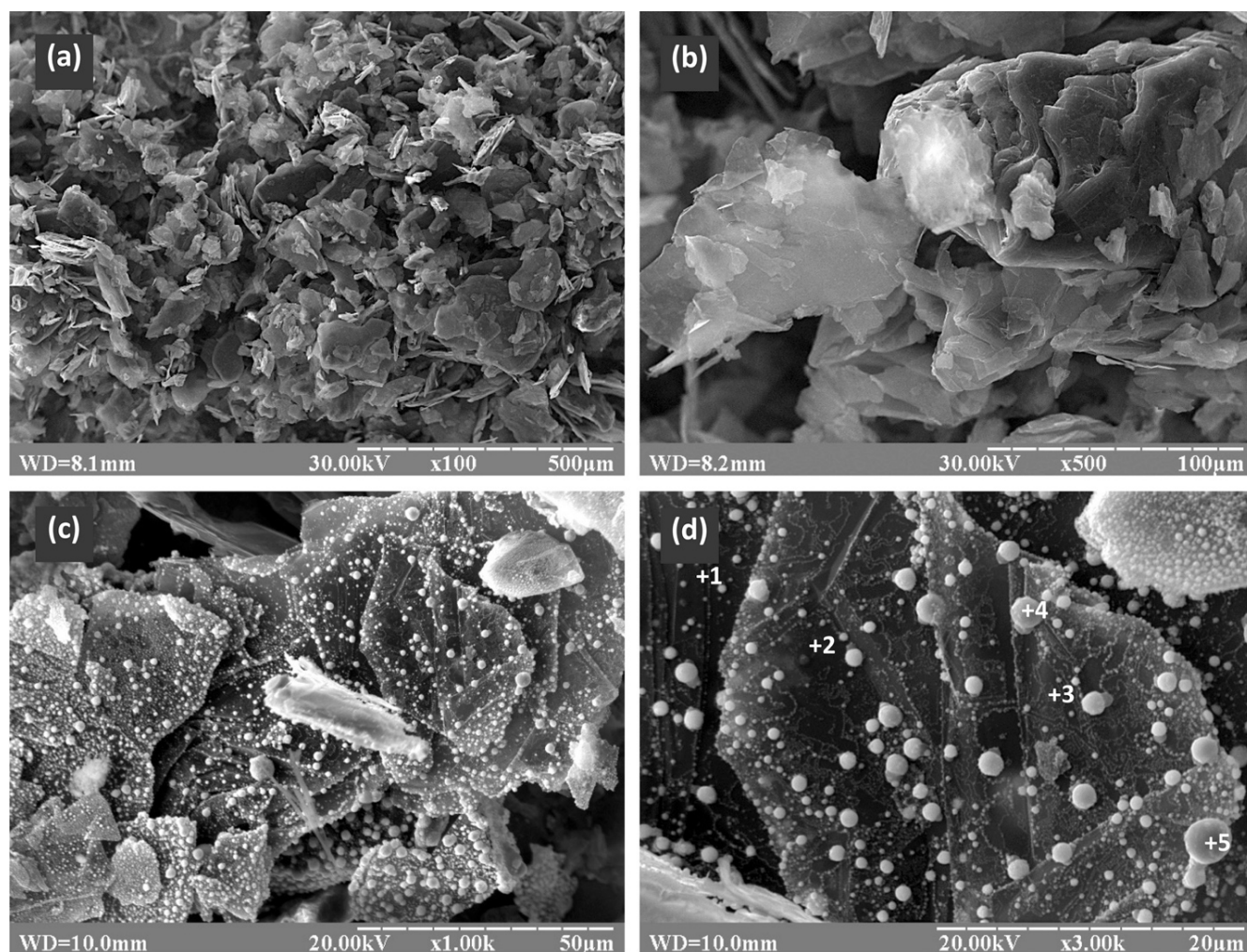


Fig. 4. SEM images of the nanostructures found in Zone 4 (Ref. Fig. 1b): a) general view of the exfoliated layer; b) magnified view revealing the stacked 2D microstructure; c) 2D nanostructures with a size of about 40 μm in diameter and thickness of about 50 nm covered by the nanodots; d) magnified view of the nanodots with characteristic regions marked from 1 to 5

at that, small amount of oxygen and relatively large concentration of carbon allows suggesting about the core-shell structure of the droplets, when the metal core composed of the iron-copper alloy, is covered by the carbon shell that protects the core from the oxidation.

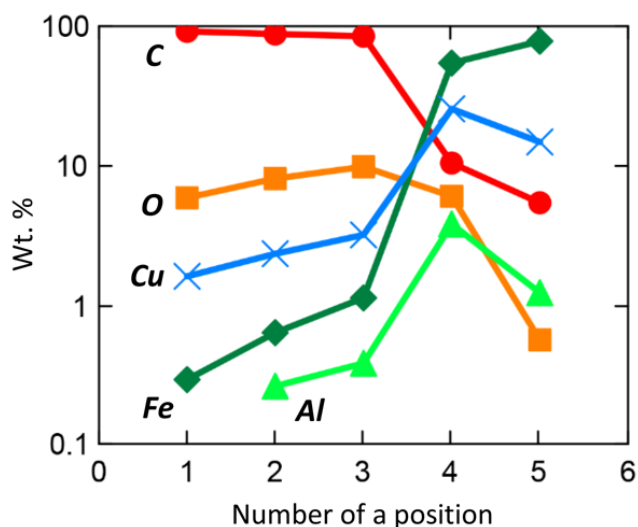


Fig. 5. Results of EDS analysis of the positions marked in Fig. 4: 1 – background region of the exfoliated powder revealing a presence of carbon (92.3%) with a small content of oxygen (5.7%) copper (1.6%), and iron (0.4%), no traces of aluminium are detected; 2 – surface of a graphite leaf with the sizes of about $30\ \mu\text{m} \times 50\ \mu\text{m}$ composed of carbon (88.8%) with a small content of oxygen (8.1%), copper (2.2%), iron (0.6%), and aluminium (0.3%); 3 – another part of the graphite leaf with almost the same content of carbon (85.4%), oxygen (9.8%) copper (3.2%), iron (1.2%), and aluminium (0.4%); 4 – microdroplet with a diameter of $2\ \mu\text{m}$ and a content of carbon (10.4%), oxygen (6.0%) copper (25.5%), iron (54.4%), and aluminium (3.7%); 5 – microdroplet with a diameter of $3\ \mu\text{m}$ and a content of carbon (5.4%), oxygen (0.6%) copper (14.8%), iron (78.0%), and aluminium (1.2%)

4. Conclusions

Implementation of arc discharge ignited at atmospheric conditions in a mixture of graphite powder with a small amount of iron and aluminium and use of copper samples as a positively biased electrode proved to be a foundation for the development of a reliable, highly productive and cost-effective technology of synthesis of metal alloy micro- and

nanoparticles. The product of the treatment is presented by the spherical structures composed of a core made of iron-copper-aluminium alloy with the iron content of 54 to 78 wt.%, which is shelled by the thin carbon layer that prevents the core from oxidation. The sizes of the particles are ranged from a few μm to a nanometre size. The particles are arranged on flat graphitic interfaces, which is beneficial for the purposes of their collection.

In future, the generated particles are considered for a catalytic application. In that case, the nanoparticles densely packed into the large two-dimensional graphitic shell that protects the metal core particles from oxidation, should undergo the action of solvents to remove the shell directly before the application the nanoparticles as active metals.

Acknowledgements

The authors acknowledge the support from the project “Scientific foundations of growth of oxide and carbon nanostructures under conditions of plasma environment” financed by the National Research Foundation of Ukraine under grant agreement No. 2020.02/0119.

References

- [1] G. Machalska, M. Noworolnik, M. Szindler, W. Sitek, R. Babilas, Titanium dioxide nanoparticles and thin films deposited by an atomization method, *Archives of Materials Science and Engineering* 100/1-2 (2019) 34-41. DOI: <https://doi.org/10.5604/01.3001.0013.6000>
- [2] A. Breus, S. Abashin, I. Lukashov, O. Serdiuk, Anodic growth of copper oxide nanostructures in glow discharge, *Archives of Materials Science and Engineering* 114/1 (2022) 24-33. DOI: <https://doi.org/10.5604/01.3001.0015.9850>
- [3] K. Szmajnta, M.M. Szindler, M. Szindler, Synthesis and magnetic properties of Fe_2O_3 nanoparticles for hyperthermia application, *Archives of Materials Science and Engineering* 109/2 (2021) 80-85. DOI: <https://doi.org/10.5604/01.3001.0015.2627>
- [4] M. Szindler, M.M. Szindler, L.A. Dobrzański, T. Jung, NiO nanoparticles prepared by the sol-gel method for a dye sensitized solar cell applications, *Archives of Materials Science and Engineering* 92/1 (2018) 15-21. DOI: <https://doi.org/10.5604/01.3001.0012.5507>
- [5] K. Loza, M. Heggen, M. Epple, Synthesis, Structure, Properties, and Applications of Bimetallic

- Nanoparticles of Noble Metals, *Advanced Functional Materials* 30/21 (2020) 1909260.
DOI: <https://doi.org/10.1002/adfm.201909260>
- [6] V. Ruzaikin, I. Lukashov, Experimental method of ammonia decomposition study based on thermal-hydraulic approach, *Results in Engineering* 15 (2022) 100600.
DOI: <https://doi.org/10.1016/j.rineng.2022.100600>
- [7] V. Ruzaikin, I. Lukashov, T. Fedorenko, S. Abashin, The equilibrium contact angle of ammonia-stainless steel interface, *Results in Engineering* 16 (2022) 100691.
DOI: <https://doi.org/10.1016/j.rineng.2022.100691>
- [8] W. Zhu, X. Dong, H. Huang, M. Qi, Iron nanoparticles-based magnetorheological fluids: A balance between MR effect and sedimentation stability, *Journal of Magnetism and Magnetic Materials* 491 (2019) 165556.
DOI: <https://doi.org/10.1016/j.jmmm.2019.165556>
- [9] M. Nasrollahzadeh, M. Sajjadi, H.A. Khonakdar, Synthesis and characterization of novel Cu(II) complex coated Fe₃O₄@SiO₂ nanoparticles for catalytic performance, *Journal of Molecular Structure* 1161 (2018) 453-463.
DOI: <https://doi.org/10.1016/j.molstruc.2018.02.026>
- [10] H. Wu, D. Lan, B. Li, L. Zhang, Y. Fu, Y. Zhang, H. Xing, High-entropy alloy@air@Ni–NiO core-shell microspheres for electromagnetic absorption applications, *Composites Part B: Engineering* 179 (2019) 107524. DOI: <https://doi.org/10.1016/j.compositesb.2019.107524>
- [11] O. Gnytko, A. Kuznetsova, Theoretical research of the chip removal process in milling of the closed profile slots, *Archives of Materials Science and Engineering* 113/2 (2022) 69-76.
DOI: <https://doi.org/10.5604/01.3001.0015.7019>
- [12] O. Shorinov, Finite element analysis of thermal stress in Cu₂O coating synthesized on Cu substrate, *Archives of Materials Science and Engineering* 115/2 (2022) 58-65.
DOI: <https://doi.org/10.5604/01.3001.0016.0753>
- [13] J.M. Lee, R.C. Miller, L.J. Moloney, A.L. Prieto, The development of strategies for nanoparticle synthesis: Considerations for deepening understanding of inherently complex systems, *Journal of Solid State Chemistry* 273 (2019) 243-286.
DOI: <https://doi.org/10.1016/j.jssc.2018.12.053>
- [14] O. Baranov, M. Košiček, G. Filipič, U. Cvelbar, A deterministic approach to the thermal synthesis and growth of 1D metal oxide nanostructures, *Applied Surface Science* 566 (2021) 150619. DOI: <https://doi.org/10.1016/j.apsusc.2021.150619>
- [15] A. Breus, S. Abashin, O. Serdiuk, Carbon nanostructure growth: new application of magnetron discharge, *Journal of Achievements in Materials and Manufacturing Engineering* 109/1 (2021) 17-25. DOI: <https://doi.org/10.5604/01.3001.0015.5856>
- [16] O. Baranov, M. Romanov, J. Fang, U. Cvelbar, K. Ostrikov, Control of ion density distribution by magnetic traps for plasma electrons, *Journal of Applied Physics* 112/7 (2012) 073302.
DOI: <https://doi.org/10.1063/1.4757022>
- [17] Y. Wang, W. Wang, J. Sun, C. Sun, Y. Feng, Z. Li, Microwave-based preparation and characterization of Fe-cored carbon nanocapsules with novel stability and super electromagnetic wave absorption performance, *Carbon* 135 (2018) 1-11.
DOI: <https://doi.org/10.1016/j.carbon.2018.04.026>
- [18] O. Baranov, G. Filipič, U. Cvelbar, Towards a highly-controllable synthesis of copper oxide nanowires in radio-frequency reactive plasma: fast saturation at the targeted size, *Plasma Sources Science and Technology* 28/8 (2019) 084002.
DOI: <https://doi.org/10.1088/1361-6595/aae12e>
- [19] O.O. Baranov, J. Fang, A.E. Rider, S. Kumar, K. Ostrikov, Effect of ion current density on the properties of vacuum arc-deposited TiN coatings, *IEEE Transactions on Plasma Science* 41/12 (2013) 3640-3644.
DOI: <https://doi.org/10.1109/TPS.2013.2286405>
- [20] A.A. Ashkarran, S.M. Aghigh, S.A.A. Afshar, M. Kavani-pour, M. Ghoranneviss, Synthesis and Characterization of ZrO₂ Nanoparticles by an Arc Discharge Method in Water, *Synthesis and Reactivity in Inorganic, Metal-Organic, and Nano-Metal Chemistry* 41/5 (2011) 425-428.
DOI: <https://doi.org/10.1080/15533174.2011.568423>
- [21] A.A. Ashkarran, B. Mohammadi, ZnO nanoparticles decorated on graphene sheets through liquid arc discharge approach with enhanced photocatalytic performance under visible-light, *Applied Surface Science* 342 (2015) 112-119.
DOI: <https://doi.org/10.1016/j.apsusc.2015.03.030>
- [22] S.B. Tharchanaa, K. Priyanka, K. Preethi, G. Shanmugavelayutham, Facile synthesis of Cu and CuO nanoparticles from copper scrap using plasma arc discharge method and evaluation of antibacterial activity, *Materials Technology* 36/2 (2021) 97-104. DOI: <https://doi.org/10.1080/10667857.2020.1734721>

- [23] J.P. Lei, X.L. Dong, X.G. Zhu, M.K. Lei, H. Huang, X.F. Zhang, B. Lu, W.J. Park, H.S. Chung, Formation and characterization of intermetallic Fe-Sn nanoparticles synthesized by an arc discharge method, *Intermetallics* 15/12 (2007) 1589-1594. DOI: <https://doi.org/10.1016/j.intermet.2007.06.010>
- [24] C. Wang, P. Zhai, Z. Zhang, Y. Zhou, J. Ju, Z. Shi, D. Ma, R.P.S. Han, F. Huang, Synthesis of Highly Stable Graphene-Encapsulated Iron Nanoparticles for Catalytic Syngas Conversion, *Particle and Particle Systems Characterization* 32/1 (2015) 29-34. DOI: <https://doi.org/10.1002/ppsc.201400039>
- [25] P.Z. Si, C.J. Choi, E. Bruck, D.Y. Geng, Z.D. Zhang, Structure and magnetic properties of surface alloyed Fe nanocapsules prepared by arc discharge, *Physica B: Condensed Matter* 369/1-4 (2005) 215-220. DOI: <https://doi.org/10.1016/j.physb.2005.08.023>
- [26] X. Qu, Y. Zhou, X. Li, M. Javid, F. Huang, X. Zhang, X. Dong, Z. Zhang, Nitrogen-doped graphene layer-encapsulated NiFe bimetallic nanoparticles synthesized by an arc discharge method for a highly efficient microwave absorber, *Inorganic Chemistry Frontiers* 7/5 (2020) 1148-1160. DOI: <https://doi.org/10.1039/c9qi01577a>
- [27] Q. Tan, L. Tao, S.U. Rehman, M. Zhong, L. Wang, C. Chen, H. Xiong, W. Xie, Z. Zhong, Improved microwave absorbing properties of core-shell FeCo@C nanoparticles, *Materials Research Express* 6/7 (2019) 075034. DOI: <https://doi.org/10.1088/2053-1591/ab1561>
- [28] D. Bera, S.C. Kuiry, M. McCutchen, A. Kruize, H. Heinrich, M. Meyyappan, S. Seal, In-situ synthesis of palladium nanoparticles-filled carbon nanotubes using arc-discharge in solution, *Chemical Physics Letters* 386/4-6 (2004) 364-368. DOI: <https://doi.org/10.1016/j.cplett.2004.01.082>
- [29] P.K. Karahaliou, P. Svarnas, S.N. Georga, N.I. Xanthopoulos, D. Delaportas, C.A. Krontiras, I. Alexandrou, CuO/Ta₂O₅ core/shell nanoparticles synthesized in immersed arc-discharge: production conditions and dielectric response, *Journal of Nanoparticle Research* 14 (2012) 1297. DOI: <https://doi.org/10.1007/s11051-012-1297-3>
- [30] B. Xu, J. Guo, X. Wang, X. Liu, H. Ichinose, Synthesis of carbon nanocapsules containing Fe, Ni or Co by arc discharge in aqueous solution, *Carbon* 44/13 (2006) 2631-2634. DOI: <https://doi.org/10.1016/j.carbon.2006.04.024>
- [31] M. Bystrzejewski, O. Łabędź, W. Kaszuwara, A. Huczko, H. Lange, Controlling the diameter and magnetic properties of carbon-encapsulated iron nanoparticles produced by carbon arc discharge, *Powder Technology* 246 (2013) 7-15. DOI: <https://doi.org/10.1016/j.powtec.2013.04.052>
- [32] A.M. El-khatib, I.I. Bondouk, Kh.M. Omar, Ah. Hamdy, M. El-khatib, Impact of changing electrodes dimensions and different ACs on the characteristics of nano composites NZnO/MWCNTs prepared by the arc discharge method, *Surfaces and Interfaces* 29 (2022) 101736. DOI: <https://doi.org/10.1016/j.surfin.2022.101736>
- [33] S. Hinokuma, S. Misumi, H. Yoshida, M. Machida, Nanoparticle catalyst preparation using pulsed arc plasma deposition, *Catalysis Science and Technology* 5/9 (2015) 4249-4257. DOI: <https://doi.org/10.1039/c5cy00636h>
- [34] Y.-C. Huang, M.-H. Teng, T.-H. Tsai, A new model for the synthesis of graphite encapsulated nickel nanoparticles when using organic compounds in an arc-discharge system, *Diamond and Related Materials* 103 (2020) 107719. DOI: <https://doi.org/10.1016/j.diamond.2020.107719>
- [35] R. Kuchi, H.M. Nguyen, V. Dongquoc, P.C. Van, S. Surabhi, S.-G. Yoon, D. Kim, J.-R. Jeong, In-Situ Co-Arc Discharge Synthesis of Fe₃O₄/SWCNT Composites for Highly Effective Microwave Absorption, *Physica Status Solidi A* 215/20 (2018) 1700989. DOI: <https://doi.org/10.1002/pssa.201700989>
- [36] X. Liu, L. Yu, F. Liu, L. Sheng, K. An, H. Chen, X. Zhao, Preparation of Ag-Fe-decorated single-walled carbon nanotubes by arc discharge and their antibacterial effect, *Journal of Materials Science* 47 (2012) 6086-6094. DOI: <https://doi.org/10.1007/s10853-012-6523-y>
- [37] A. Mao, H. Xiang, X. Ran, Y. Li, X. Jin, H. Yu, X. Gu, Plasma arc discharge synthesis of multicomponent Co-Cr-Cu-Fe-Ni nanoparticles, *Journal of Alloys and Compounds* 775 (2019) 1177-1183. DOI: <https://doi.org/10.1016/j.jallcom.2018.10.170>
- [38] O. Baranov, M. Romanov, Process intensification in vacuum arc deposition setups, *Plasma Processes and Polymers* 6/2 (2009) 95-100. DOI: <https://doi.org/10.1002/ppap.200800131>
- [39] C. Wang, Z. Lu, D. Li, W. Xia, W. Xia, Effect of the Magnetic Field on the Magnetically Stabilized Gliding

Arc Discharge and Its Application in the Preparation of Carbon Black Nanoparticles, Plasma Chemistry and Plasma Processing 38 (2018) 1223-1238. DOI: <https://doi.org/10.1007/s11090-018-9915-1>

[40] C. Wang, D. Li, Z. Lu, M. Song, W. Xia, Synthesis of carbon nanoparticles in a non-thermal plasma process, Chemical Engineering Science 227 (2020) 115921. DOI: <https://doi.org/10.1016/j.ces.2020.115921>



© 2023 by the authors. Licensee International OCSCO World Press, Gliwice, Poland. This paper is an open-access paper distributed under the terms and conditions of the Creative Commons Attribution-NonCommercial-NoDerivatives 4.0 International (CC BY-NC-ND 4.0) license. (<https://creativecommons.org/licenses/by-nc-nd/4.0/deed.en>).